RSC Advances

ROYAL SOCIETY OF CHEMISTRY

www.rsc.org/advances

RSC Advances

PAPER

Degradation and Nano-Patterning of Ferroelectric P(VDF-TrFE) Thin Films with Electron Irradiation

Ren Zhu, Kory Jenkins, and Rusen Yang*

Received 00th January 20xx,
Accepted 00th January 20xx

DOI: 10.1039/x0xx00000x

www.rsc.org/

P(VDF-TrFE) nanofilm is a critical component in many organic electronics. Here we report the irreversible degradation of its ferroelectricity due to medium-energy electron irradiation (< 10 keV), which is commonly found in device fabrication and characterization tools. The first-order electromechanical coupling in P(VDF-TrFE) was directly measured by atomic force microscopy to study the ferroelectricity switching property. Results showed that P(VDF-TrFE) films became non-ferroelectric after metal deposition in an electron-beam evaporator or after two minutes of observation under a scanning electron microscope. Lowering the electron energy slowed down the degradation process, but 500 eV electrons were still detrimental to the film. Irradiation is believed to transform the *all-trans* polar phase of P(VDF-TrFE) into a non-polar state, as revealed by infrared spectroscopy. On the other hand, controlled electron irradiation allows us to create patterns on the ferroelectric P(VDF-TrFE) thin films at submicron spatial resolution.

Introduction

Poly(vinylidene fluoride) (PVDF) is a semicrystalline polymer with at least four different chain conformations, named α, β, γ, and δ phase. β-phase PVDF has an *all-trans* structure (TTT), and the big difference in the electronegativity between hydrogen and fluorine results in a strong dipole moment normal to the chain direction. The polar β-phase is ferroelectric, and when poled, its piezoelectric property is the strongest among common ferroelectric polymers.[1, 2] Compared with perovskite ceramics, PVDF has a large piezoelectric voltage constant, low acoustic impedances in fluids, and excellent chemical resistance, flexibility, processability, and dielectric breakdown strength.[3]

PVDF films processed from melting are mostly α-phase,[4] which has an alternating *trans-gauche* (TGTG') conformation and is not ferroelectric. Films from solution casting can also contain a large fraction of α-phase unless solvent polarity and process temperature are optimized.[5, 6] However, its random copolymer poly(vinylidene fluoride-trifluoroethylene) [P(VDF-TrFE)] readily forms β-phase from melting or solution, because the incorporation of TrFE as defects in the VDF chains makes the β-phase more energetically favorable.[7] Moreover, P(VDF-TrFE) with a proper VDF content has better crystallinity, higher remnant polarization, and lower coercive field than PVDF.[2] Various novel devices have been fabricated from solution-processed P(VDF-TrFE) thin films, particularly organic non-volatile memories (NVM) based on ferroelectric capacitors, transistors, or diodes.[8, 9]

It is well known that electron irradiation changes the structure and property of PVDF and its copolymers.[10-27] For instance, Lovinger observed that under 100 keV electron irradiation β-P(VDF-TrFE) first transformed into an intermediate phase which was structurally analogous to a paraelectric lattice, and then degraded to an amorphous structure.[10] Zhang *et al.* found that after exposure in 3 MeV electrons, P(VDF-TrFE) exhibited a slim polarization hysteresis loop and some other features that were in common with relaxor ferroelectrics.[15] Most studies showed a decrease in the crystallinity after irradiation, but an opposite trend was also reported.[13]

The electron beams (e-beams) used in previous studies all had very high energy, in the range between 100 keV and several MeV. Such harsh radiation is not common in the normal manufacturing facilities or working environments of PVDF-based devices. On the other hand, electron sources with energy below 50 keV can be found in many fabrication and characterization tools, such as scanning electron microscopy (SEM), e-beam evaporation, e-beam lithography, Auger electron spectroscopy, *etc.* As the electron energy decreases, the penetration becomes shallower. The maximum range of a 10 keV e-beam in P(VDF-TrFE) is only about 2 μm,[28] which may not be a concern for thick films. However, in the recent development of ferroelectric memories, P(VDF-TrFE) films need to be thinner than 100 nm in order to bring the switching voltage below 10 V.[29, 30] Thus it becomes imperative to understand the effect of medium-energy electron irradiation on ferroelectric property of ultrathin P(VDF-TrFE) films.

Department of Mechanical Engineering, University of Minnesota, Minneapolis, MN 55414, USA
E-Mail: yangr@umn.edu
† Footnotes relating to the title and/or authors should appear here.
Electronic Supplementary Information (ESI) available. See DOI: 10.1039/x0xx00000x

In this paper, we used an atomic force microscope (AFM) to study the domain switching in P(VDF-TrFE). After exposure to 8 keV electrons in an e-beam evaporator or an SEM, films were no longer switchable, indicating the loss of ferroelectricity. Effect of exposure time and electron energy was investigated, and microstructural change in irradiated film was characterized by Fourier transform infrared spectroscopy (FTIR). Finally, the patterning of ferroelectric property in a P(VDF-TrFE) film by controlled electron irradiation was demonstrated.

Experimental Section

Fabrication of P(VDF-TrFE) film

P(VDF-TrFE) copolymer powder (70/30 mol%, Piezotech, France) was thoroughly dissolved in cyclohexanone with a concentration of 33 mg/mL. Substrates were prepared by depositing 60 nm Au onto small pieces of a Si wafer. P(VDF-TrFE) film was coated on the substrate by spinning the solution at 4000 rpm for 1 min, on a home-made spin-coater placed in a 60 °C oven. Spin-coating at an elevated temperature improves the solubility of P(VDF-TrFE) in cyclohexanone and helps reduce the roughness of the film. Then the film was baked on a 135 °C hotplate shortly to remove residual solvent. To improve its crystallinity, the film was baked in a 135 °C oven under vacuum for 1 hour, which is above its Curie temperature (106 °C) but below its melting point (151 °C). Finally the film was slowly cooled down to room temperature. The film thickness was about 80-100 nm, as determined by AFM and SEM.

Poling and characterization of P(VDF-TrFE) by AFM

The AFM is an MFP-3D from Asylum Research, and the probe is an ASYELEC-01 from Asylum Research, which has a spring constant of about 2 N/m and an iridium conductive coating. To pole the P(VDF-TrFE) film, the bottom Au electrode of the sample was grounded, and the probe was biased at either +15 V or -15 V. Then the probe scanned the film in a contact mode, with a rate of 12 μm/sec.

For the PFM characterization of the film, the bottom Au electrode was grounded, and a 20 kHz 4 V sinusoidal voltage was applied on the conductive probe. Higher voltage amplitude of up to 7 V had been tried. Similar to the poling process, the probe scanned the film in a contact mode, with a rate of 12 μm/sec. The electric field is below the coercive field of the P(VDF-TrFE) film, and the exciting frequency of 20 kHz was below the contact resonance frequency between the film and the probe, which was above 100 kHz.

E-beam evaporation and SEM

The e-beam evaporator is an SEC-600 from CHA Industries. During the Au deposition, the chamber pressure was below 1.5×10^{-6} Torr, the acceleration voltage was fixed at 8 kV, and emission current was automatically controlled to give the desired deposition rate. For a deposition rate of 1 Å/sec, a typical emission current was 60 mA.

The SEM is a JSM-6700F from JEOL, which has a field emission gun. During all the tests, the chamber pressure was below 3.0×10^{-6} Torr, the emission current from the gun was 10 μA, and the probe current reaching the sample was set to an index of 13, which is about 1 nA according to the operation manual of the SEM. The acceleration voltage was varied between 500 V and 8 kV in different tests, and after each adjustment, the gun was aligned to maximize the brightness of image, and the aperture and the stigmators were also aligned. When collecting the data in Fig. 2 and Fig. 3, we set the SEM magnification to be 300×, which gave a scan area of about 400 μm by 288 μm. In Fig. 5, the SEM magnification was 250×.

Results and Discussion

P(VDF-TrFE) film was spin-coated on a Si/Au substrate, followed by annealing above its Curie point to increase crystallinity and content of β-phase.[31] Topography image shows a smooth surface with nano-size crystalline grains (Fig. S1†). As-coated P(VDF-TrFE) has domains with different polar directions, and needs a poling process to align the dipoles in order to exhibit piezoelectricity. We biased the conductive AFM probe at 15 V with respect to the bottom Au electrode and scanned the film with very small contact force. Since the film thickness was only 80-100 nm, the electric field in between was above the coercive field of P(VDF-TrFE) and forced the dipole moment into the out-of-plane direction. Using the AFM probe to perform the poling eliminated the need for depositing top electrodes and avoided variations introduced by metallization processes.

After poling, we used piezoresponse force microscopy (PFM) to study the ferroelectric effect in P(VDF-TrFE). PFM only extracts the first-order electromechanical coupling from piezoelectricity. Irradiated P(VDF-TrFE) may exhibit exceptionally high electrostrictive strain in an electric field,[15, 17, 24, 26] which is irrelevant to ferroelectric NVM or sensor applications. Fortunately, electrostriction is a second-order effect, so our PFM measurements could reject its response with a lock-in amplifier.

Fig. 1a and b show the PFM amplitude map and phase map of a new P(VDF-TrFE) film after poling. Region I in the image was original film without poling and had random dipoles. The piezoresponse of those small domains cancelled each other, resulting in low PFM amplitude and noisy PFM phase. Region II and III were poled by the AFM at +15 V and -15 V probe respectively. As expected, they had much higher PFM amplitude than Region I. In addition, Region II and II had a phase difference of about 180°, which is due to the opposite polar orientations of the two regions. A positive bias caused Region III to expand but Region II to contract. The ferroelectric hysteresis of P(VDF-TrFE) was characterized by PFM and showed in Fig. S2†.

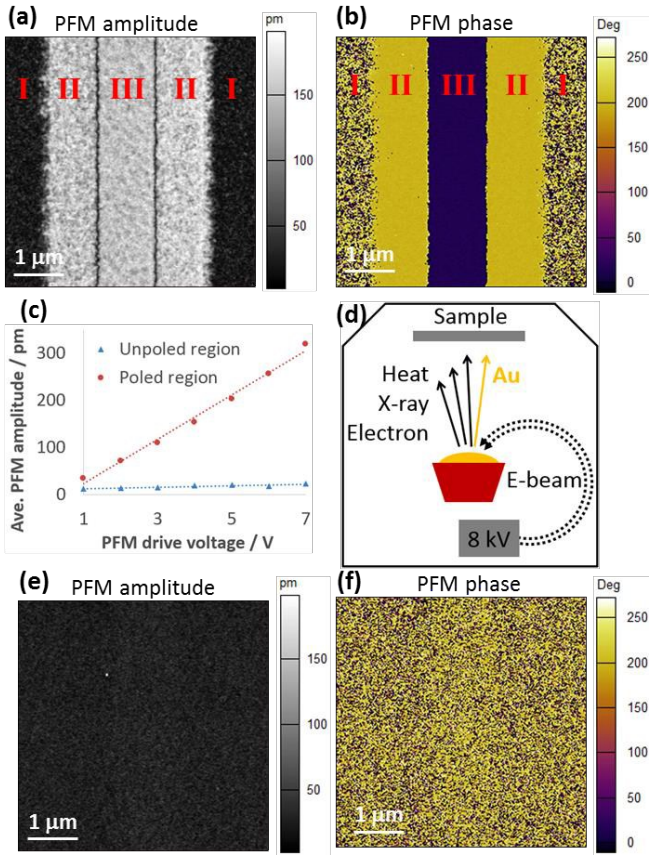

Fig. 1. PFM characterization of P(VDF-TrFE) films before and after e-beam evaporation. (a, b) PFM amplitude and phase of a new P(VDF-TrFE) film. Region I was not poled, while Region II and III were poled by + 15 V and -15 V respectively. Scan size was 5 μm by 5 μm. The same poling and PFM procedure was applied to obtain images in Fig. 1, 2, and 3. (c) Average PFM amplitude in the poled region (red circle) and unpoled region (blue triangle) as the drive voltage was varied. (d) Illustration of the e-beam evaporation process and its possible impact on the P(VDF-TrFE) film. (e, f) PFM amplitude and phase of a P(VDF-TrFE) film after e-beam evaporation.

In PFM, both electromechanical and electrostatic interactions can contribute to the probe oscillation at the frequency of the drive voltage.[32] The electrostatic effect comes from the probe-sample capacitance. To verify that the PFM signal was mainly from the piezoelectricity rather than the capacitance, we tested different PFM drive voltages on both poled and unpoled areas of the film. In Fig. 1c, the average PFM amplitude on the non-piezoelectric part of the film stayed low, indicating that the electrostatic interaction was not significant. In contrast, the vibration amplitude increased with the drive voltage in the poled area. The linear fit of the data gives an effective d_{33} coefficient of 47 pm/V, and the high piezoelectric coefficient confirmed the high quality of the as-grown film. Therefore, probe oscillation was predominantly from the electromechanical interaction, and as-prepared P(VDF-TrFE) films had excellent ferroelectric property.

In most electronic device structures, there are metal electrodes on top of the ferroelectric film deposited either by evaporation or sputtering.[8] We deposited 60 nm Au via e-beam evaporation on a P(VDF-TrFE) film, and then removed the Au by a wet etchant (aqueous solution of potassium iodide and iodine). The etchant itself does not attack P(VDF-TrFE), so any change in the property of the film must have been due to the metal evaporation process (Fig. S3†). As illustrated in Fig. 1d, in the e-beam evaporator, electrons are accelerated by a voltage of 8 kV to bombard the Au target. Interaction between electrons and Au not only generates heat that vaporizes the metal, but also induces 2.1 keV characteristic x-ray [33] and 8 keV backscattered electrons (BSE), both being ionizing radiation. Fig. 1e and f show the PFM maps of a P(VDF-TrFE) film after Au deposition and etching. The film was poled by the same procedure as that in Fig. 1a and b. Clearly, there is no contrast in the PFM amplitude and phase images, suggesting that the ferroelectricity was lost. Another experiment with a thermal evaporator showed that neither the heat nor the Au atom flux in the metal evaporation process affected the ferroelectric property (Fig. S4†). Therefore, the damage was due to the BSE and/or the x-ray from the e-beam. In general, the fraction of BSE increases with the atomic number of the matter. Since Au is a heavy atom, nearly half of the incident 8 keV electrons could be backscattered away from Au,[34] and some of them may reach the film. The adverse effect of electron irradiation has been confirmed with SEM and will be discussed in details. On the other hand, the role of the x-ray in the degradation of the P(VDF-TrFE) film is not fully understood at this moment (Fig. S5†). Note that the lost ferroelectricity of the P(VDF-TrFE) film could not be recovered upon long-term annealing above its paraelectric phase transition temperature. Such irreversibility suggests that irradiation had changed the chemical bonds.[21, 22]

SEM uses focused e-beam to characterize the morphology and chemical composition of materials. The electron energy is much lower than that in a transmission electron microscope,[10] but may still damage the nanometer-thick P(VDF-TrFE) film. Fig. 2 shows the PFM test of a P(VDF-TrFE) film after being scanned in SEM with 8 kV acceleration voltage and approximately 1 μA/cm^2 beam current density. In Fig. 2a and b, after only 1 min of observation under SEM, the PFM amplitude became significantly lower and the PFM phase less uniform. In Fig. 2c and d, 5 min of exposure caused the complete loss of ferroelectric property in the nanometer-thick film. For more quantitative comparison, we have calculated the average PFM amplitude in the poled area among samples with different durations of exposure in SEM. As shown in Fig. 2e, after 1 min, the PFM amplitude was reduced by half. And beyond 2 min, it dropped to a level similar to the PFM amplitude of an intact but unpoled P(VDF-TrFE) film (Fig. 1c, blue line). In Fig. 2e we also repeated the PFM test on the same group of samples at different times. After one week, the PFM amplitude did not change much in most samples, implying that the damage from the SEM is not a transient effect from trapped charges.

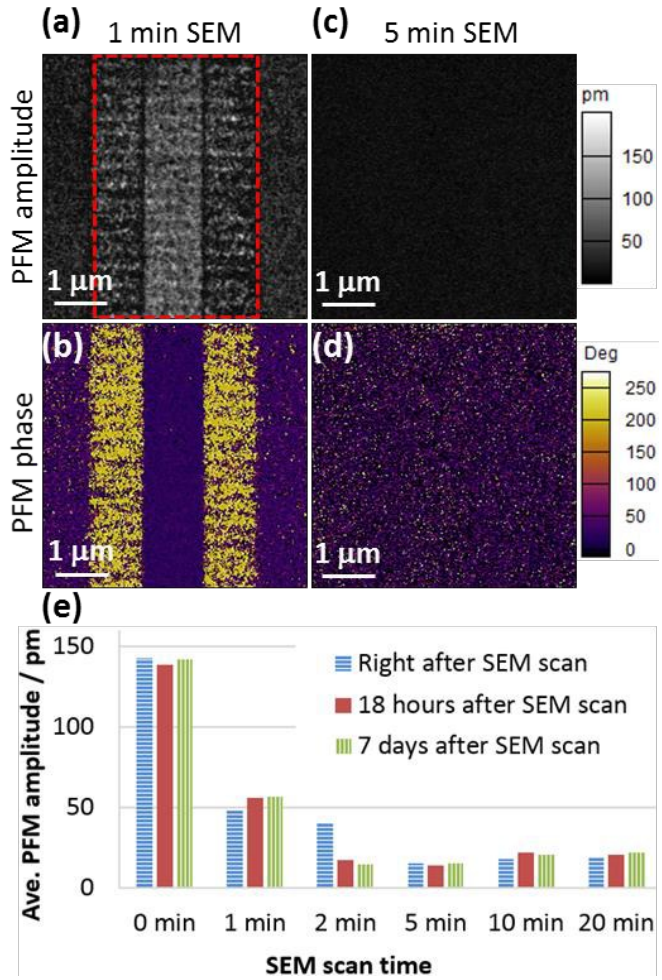

Fig. 2. (a, b) PFM amplitude and phase of P(VDF-TrFE) films with 1 min electron irradiation in SEM. (c, d) PFM amplitude and phase of P(VDF-TrFE) films with 5 min electron irradiation in SEM. (e) Average PFM amplitude in the poled area. Six samples with different electron exposure in SEM were scanned. The tests were conducted right after the exposure, and then repeated after 18 hours and 7 days. The poled area was indicated by a red dashed box in (a).

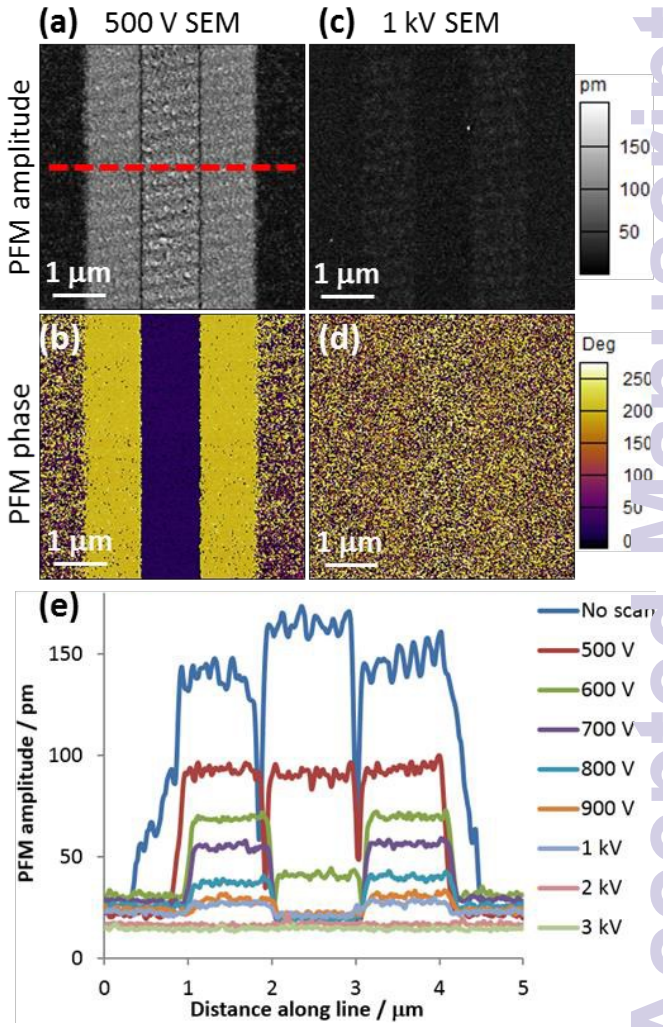

Fig. 3. (a, b) PFM amplitude and phase of P(VDF-TrFE) films with 500 eV electron irradiation in SEM. (c, d) PFM amplitude and phase of P(VDF-TrFE) films with 1 keV electron irradiation in SEM. (e) Horizontal section lines of PFM amplitude images from 9 samples. Samples were scanned by SEM with different acceleration voltages. The section line is indicated by a red dashed line in (a).

Comparing Fig. 2d and Fig. 1f, we notice that the phase map in Fig. 1f is a random mixture of different phases, while the phase in Fig. 2d is mostly around 0°. The data in Fig. 2d was obtained immediately after the SEM treatment, and the dominating phase around 0° might have been related to the electrostatic effect from electrons captured by the film.[35] Even if the trapped charge contributed to the probe-sample interaction, the influence was weak, as evidenced by the small PFM amplitude signal. One week after the SEM treatment, PFM phase of the same sample became similar to Fig. 1f (data shown in Fig. S6†), probably because the trapped charges had dissipated.

In SEM the electron energy is adjustable. The question then arises as to whether the damage on P(VDF-TrFE) can be avoided by using a lower acceleration voltage. We have experimented with different voltages down to 500 V, which is the lower limit of our SEM. The exposure time was kept as 5 min and the electron flux as 1 μA/cm^2. In Fig. 3a and b, a P(VDF-TrFE) film exposed in 500 V e-beam still gave clear contrast in the PFM image. However in Fig. 3c and d, as the electron energy increased to 1 keV, the damage was much more severe and little ferroelectricity remained in the film. Horizontal section lines of PFM amplitude from different samples are plotted in Fig. 3e. 500 eV electron irradiation reduced the PFM amplitude in the poled area by almost 50%. Therefore, ferroelectricity of the P(VDF-TrFE) thin film is sensitive to even very low-energy electrons. When the electron energy is above 2 keV, the PFM section line becomes flat, which means there is no difference between the poled area and the unpoled area, and the film was no longer switchable.

To understand the structural change in irradiated P(VDF-TrFE) nanofilms, we characterized the film before and after e-beam evaporation by vibrational spectroscopy. Fig. 4 shows the FTIR spectra of P(VDF-TrFE) films in the frequency range of 1600-700 cm^{-1}. This range contains many infrared absorption bands related to the heavy fluorine atoms,[36] and they had the most significant change after electron irradiation.[19] Decreases in the intensity of most bands suggest that e-beam might have reduced the content of fluorine. This agrees with the finding of Macchi *et al.* that e-beam caused hydrogen fluoride desorption in P(VDF-TrFE).[27] Among those bands, 854 cm^{-1} is assigned to the symmetric CF_2 stretching, and 1298 cm^{-1} is assigned to the symmetric CF_2 stretching coupled with skeletal CC stretching.[37, 38] Both bands are the characteristics of long *trans* sequences, and they diminished after e-beam evaporation. Therefore, FTIR data confirms the absence of the *all-trans* β-phase in irradiated P(VDF-TrFE) nanofilms.

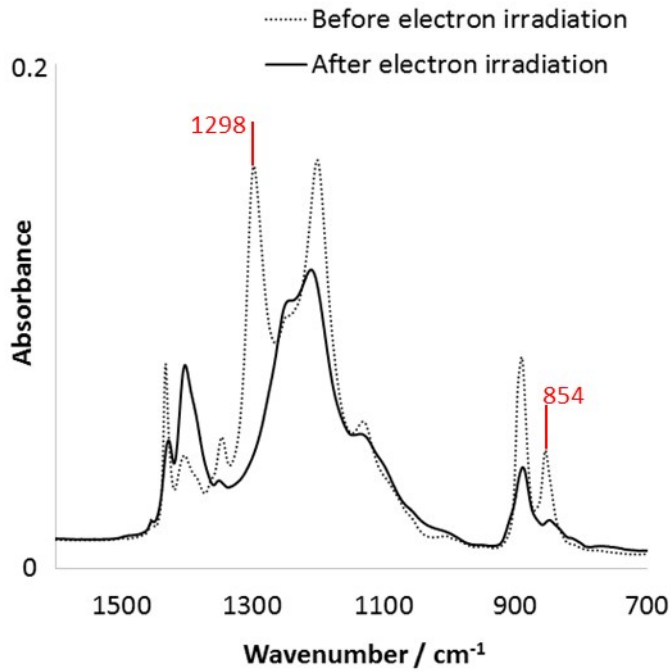

Fig. 4. FTIR spectrum of an intact film and a film after e-beam evaporation.

Because electron irradiation can transform the β-phase of P(VDF-TrFE) into a non-polar state, we can utilize e-beam as a lithography tool to locally manipulate the ferroelectric, piezoelectric, and pyroelectric properties of a P(VDF-TrFE) film. Kang *et al.* applied localized pressure (nanoimprint) on an α-PVDF film to obtain arrays of γ-phase domains embedded in the α-phase matrix, and such patterning is believed to be beneficial for high-density ferroelectric memory because the non-polar matrix can improve the device isolation.[39] However the nanoimprint method significantly increased the surface roughness of the film, and γ-phase has weaker ferroelectric property than β-phase. Here electron irradiation can pattern β-phase P(VDF-TrFE) without changing its surface morphology. It is also noteworthy that the P(VDF-TrFE) film can be varied continuously between non-ferroelectric and strongly ferroelectric, controlled by exposure time in Fig. 2 or by electron energy in Fig. 3. Therefore, 'grayscale lithography' is feasible.

To demonstrate the lithography with electron irradiation, we put a fine TEM grid as a shadow mask on top of a P(VDF-TrFE) film, and then scanned the film in SEM for 15 min with 500 V acceleration voltage. As shown in Fig. 5a, the area with large PFM amplitude corresponds to the region protected by the TEM grid, and the area with lower PFM amplitude was exposed to electrons through the open space on the TEM grid. Fig. 5b is a section line on the PFM amplitude map, as indicated by a red dashed line in Fig. 5a. The area irradiated by electrons has an oscillating pattern in the PFM amplitude with a period of about 350 nm. That is due to the line-by-line scanning of e-beam in the SEM. Such a periodic pattern can also be found in Fig. 2a and 3a. Result in Fig. 5 shows that the ferroelectric domains of P(VDF-TrFE) thin film can be patterned either through a shadow mask or by e-beam direct write. Commercial e-beam lithography tools can focus e-beam to a very small area and define sub-10 nm feature, so much smaller features could be expected than those in Fig. 5.

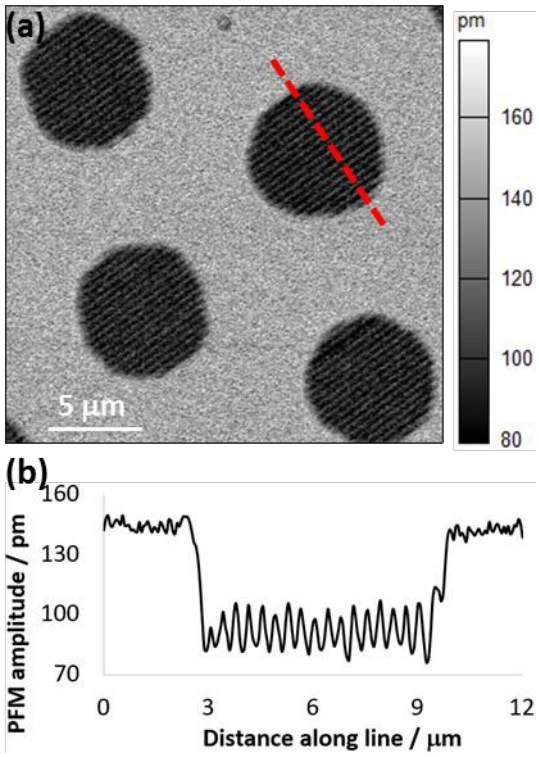

Fig. 5. E-beam patterning of a P(VDF-TrFE) film. (a) PFM amplitude map of a film scanned in SEM with a shadow mask. The whole area was poled by +15 V before PFM. The darker holes are area with poor ferroelectric property. (b) Section line on the PFM amplitude map.

Conclusions

This work demonstrates that exposure to medium-energy electron (< 10 keV) radiation has an adverse effect on the ferroelectric property of P(VDF-TrFE) nanofilms. The damage increases with absorbed dose, which depends on both exposure time and electron energy. Reducing the energy to 500 eV could

not eliminate the negative effect. Whether there exists a threshold energy below which electrons no longer attack the ferroelectric film is still under investigation. The change in the ferroelectric property of P(VDF-TrFE) is linked to the absence of the *all-trans* polar phase. Unintentional radiation damage is usually unfavorable, so alternative techniques like thermal evaporation of top electrodes and optical microscopy are recommended for the fabrication and characterization of P(VDF-TrFE) nano devices. However, controlled electron irradiation may be utilized to pattern the ferroelectric property of P(VDF-TrFE) thin films with great spatial resolution, to enable or enhance P(VDF-TrFE) applications.

Acknowledgements

The authors are truly grateful for the financial support from the Department of Mechanical Engineering and the College of Science and Engineering of the University of Minnesota. Research is also supported by NSF (ECCS-1150147). K. J. is thankful for the NSF IGERT grant (DGE-1069104). Parts of this work were carried out in the Characterization Facility, University of Minnesota, which receives partial support from NSF through the MRSEC program.

Notes and references

1 A. J. Lovinger, *Science*, 1983, **220**, 1115-1121.
2 J. S. Harrison and Z. Ounaies, in *Encyclopedia of Polymer Science and Technology*, John Wiley & Sons, Inc., 2002.
3 S. B. Lang and S. Muensit, *Appl. Phys. A-Mater.*, 2006, **85**, 125-134.
4 V. Sencadas, R. Gregorio and S. Lanceros-Méndez, *Journal of Macromolecular Science, Part B*, 2009, **48**, 514-525.
5 A. Salimi and A. A. Yousefi, *Journal of Polymer Science Part B: Polymer Physics*, 2004, **42**, 3487-3495.
6 R. Gregorio, *J. Appl. Polym. Sci.*, 2006, **100**, 3272-3279.
7 T. Furukawa, *Adv. Colloid Interface Sci.*, 1997, **71–72**, 183-208.
8 R. C. G. Naber, K. Asadi, P. W. M. Blom, D. M. de Leeuw and B. de Boer, *Adv. Mater.*, 2010, **22**, 933-945.
9 S. Ducharme, T. J. Reece, C. M. Othon and R. K. Rannow, *Device and Materials Reliability, IEEE Transactions on*, 2005, **5**, 720-735.
10 A. J. Lovinger, *Macromolecules*, 1985, **18**, 910-918.
11 A. Odajima, Y. Takase, T. Ishibashi and K. Yuasa, *Japanese Journal of Applied Physics*, 1985, **24**, 881.
12 B. Daudin, M. Dubus and J. F. Legrand, *J. Appl. Phys.*, 1987, **62**, 994-997.
13 K. D. Pae, S. K. Bhateja and J. R. Gilbert, *Journal of Polymer Science Part B: Polymer Physics*, 1987, **25**, 717-722.
14 F. Macchi, B. Daudin and J. F. Legrand, *Ferroelectrics*, 1990, **109**, 303-308.
15 Q. M. Zhang, V. Bharti and X. Zhao, *Science*, 1998, **280**, 2101-2104.
16 E. Adem, J. Rickards, G. Burillo and M. Avalos-Borja, *Radiat. Phys. Chem.*, 1999, **54**, 637-641.
17 Z.-Y. Cheng, T.-B. Xu, V. Bharti, S. Wang and Q. M. Zhang, *Appl. Phys. Lett.*, 1999, **74**, 1901-1903.
18 V. Bharti, H. S. Xu, G. Shanthi, Q. M. Zhang and K. Liang, *J. Appl. Phys.*, 2000, **87**, 452-461.
19 Z. Y. Cheng, D. Olson, H. Xu, F. Xia, J. S. Hundal, Q. M. Zhang, F. B. Bateman, G. J. Kavarnos and T. Ramotowski, *Macromolecules*, 2002, **35**, 664-672.
20 M. C. Clochard, J. Bègue, A. Lafon, D. Caldemaison, C. Bittencourt, J. J. Pireaux and N. Betz, *Polymer*, 2004, **45**, 8683-8694.
21 Z.-M. Li, S.-Q. Li and Z.-Y. Cheng, *J. Appl. Phys.*, 2005, **97**, 014102.
22 C. M. Othon, F. B. Bateman and S. Ducharme, *J. Appl. Phys.*, 2005, **98**, 014106.
23 H.-J. Ye, L. Yang, W.-Z. Shao, Y. Li, S.-B. Sun and L. Zhen, *RSC Advances*, 2014, **4**, 13525-13532.
24 V. Bharti, T. B. Xu, Z. Y. Cheng, T. Mai, Q. M. Zhang, T. Ramotowski and K. A. Wright, *Japanese Journal of Applied Physics*, 2001, **40**, 672.
25 B. Daudin, J. F. Legrand and F. Macchi, *J. Appl. Phys.*, 1991, **70**, 4037-4044.
26 Y. Tang, X.-Z. Zhao, H. L. W. Chan and C. L. Choy, *Appl. Phys. Lett.*, 2000, **77**, 1713-1715.
27 F. Macchi, B. Daudin, A. Ermolieff, S. Marthon and J. Legrand, *Radiat. Eff. Defects Solids*, 1991, **118**, 117-124.
28 K. Kanaya and S. Okayama, *J. Phys. D: Appl. Phys.*, 1972, **5**, 43.
29 A. V. Bune, V. M. Fridkin, S. Ducharme, L. M. Blinov, S. P. Palto, A. V. Sorokin, S. G. Yudin and A. Zlatkin, *Nature*, 1998, **391**, 874-877.
30 M. Li, N. Stingelin, J. J. Michels, M.-J. Spijkman, K. Asadi, R. Beerends, F. Biscarini, P. W. M. Blom and D. M. de Leeuw, *Adv. Funct. Mater.*, 2012, **22**, 2750-2757.
31 H. Kodama, Y. Takahashi and T. Furukawa, *Ferroelectrics*, 1997, **203**, 433-455.
32 S. V. Kalinin and D. A. Bonnell, *Phys. Rev. B*, 2002, **65**, 125408.
33 J. A. Bearden, *Reviews of Modern Physics*, 1967, **39**, 78-124.
34 A. Assa'd and M. El Gomati, *Scanning Microscopy*, 1998, **12**, 185-192.
35 J. Cazaux, *Microsc. Microanal.*, 2004, **10**, 670-684.
36 K. Tashiro, Y. Itoh, M. Kobayashi and H. Tadokoro, *Macromolecules*, 1985, **18**, 2600-2606.
37 K. Tashiro and M. Kobayashi, *Polymer*, 1988, **29**, 426-436.
38 N. M. Reynolds, K. J. Kim, C. Chang and S. L. Hsu, *Macromolecules*, 1989, **22**, 1092-1100.
39 S. J. Kang, Y. J. Park, J. Y. Hwang, H. J. Jeong, J. S. Lee, K. J. Kim, H. C. Kim, J. Huh and C. Park, *Adv. Mater.*, 2007, **19**, 581-586.

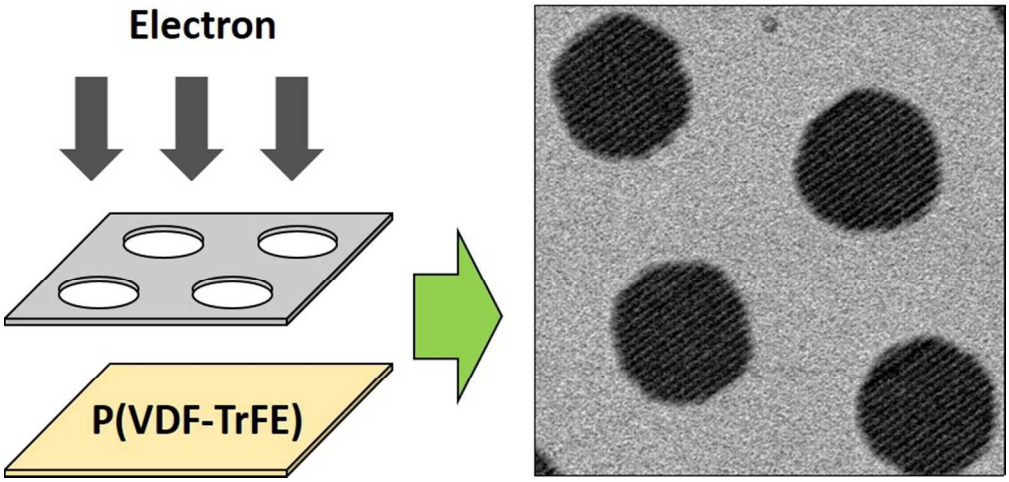

Low energy electrons were found to degrade the Ferroelectricity of P(VDF-TrFE) and a new grayscale lithography was hence proposed.
162x79mm (150 x 150 DPI)